



HISTORICAL SHORELINE CHANGE THROUGH 2007, TEXAS GULF COAST: RATES, CONTRIBUTING CAUSES, AND HOLOCENE CONTEXT

Jeffrey G. Paine, Sojan Mathew, and Tiffany Caudle

*Bureau of Economic Geology, Jackson School of Geosciences,
University of Texas at Austin, University Station, Box X, Austin, Texas 78713, U.S.A.*

ABSTRACT

Long-term historical rates of Gulf shoreline change along the Texas coast have been determined through 2007 (the latest imagery that predates Hurricane Ike) from a series of shoreline positions that includes those depicted on 1800s charts and mapped from aerial photographs, ground GPS surveys, and airborne lidar surveys. Net rates measured at 11,731 sites spaced at 164 ft (50 m) along the 332 mi (535 km) of Texas Gulf shoreline average 4.1 ft/yr (1.2 m/yr) of retreat, significantly lower than late Pleistocene to early-Holocene retreat rates of 8 to 181 ft/yr (2.4 to 55 m/yr) and similar to mid- to late Holocene rates estimated using past sea-level positions and shelf bathymetric contours as a shoreline proxy. Net shoreline retreat occurred along 84 percent of the Texas Gulf shoreline, resulting in an estimated land loss of 13,890 ac (5621 ha) since 1930 at an average rate of 180 ac/yr (73 ha/yr). Rates of change are more recessional on the upper Texas coast (-5.3 ft/yr [-1.6 m/yr] east of the Colorado River) than they are on the central and lower coast (-3.3 ft/yr [-1.0 m/yr] from the Colorado River to the Rio Grande). Rates are slightly lower than those reported through 2000, possibly reflecting lower major storm incidence and decreased relative sea-level rise rates.

Areas undergoing significant net retreat include: (1) the muddy marshes on the upper Texas coast between High Island and Sabine Pass; (2) segments on the sandy barrier-island shoreline on Galveston Island; (3) the combined fluvial/deltaic headland constructed by the Brazos and Colorado rivers; (4) sandy, headland-flanking Matagorda Peninsula west of the Colorado River; and (5) San José Island, a sandy barrier island on the central Texas coast; and (6) the northern end and much of the southern half of Padre Island, a sandy barrier island on the lower coast. Significant net shoreline advance occurred (1) adjacent to the jetties that protect dredged channels at Sabine Pass, Bolivar Roads, and Aransas Pass; (2) near tidal inlets at the western ends of Galveston Island and Matagorda Peninsula; (3) near the mouth of the Brazos River; (4) along most of Matagorda Island; and (5) on central Padre Island.

Shoreline change rates were calculated for the latest coast-wide aerial photography that predates Hurricane Ike, which struck the upper Texas coast in September 2008 and significantly altered beach and dune morphology and shoreline position. Pre-Ike photography was chosen to avoid emphasizing the nearly instantaneous effects of Ike, recognizing that significant aspects of the recovery process can continue for two or more years after a major storm. The next update of long-term shoreline change rates will be based on shoreline positions extracted from coast-wide airborne lidar data acquired in 2012.

INTRODUCTION

The Texas coastal zone (Fig. 1) is among the most dynamic environments on Earth. Shoreline position is a critical parameter

Copyright © 2012. Gulf Coast Association of Geological Societies. All rights reserved.

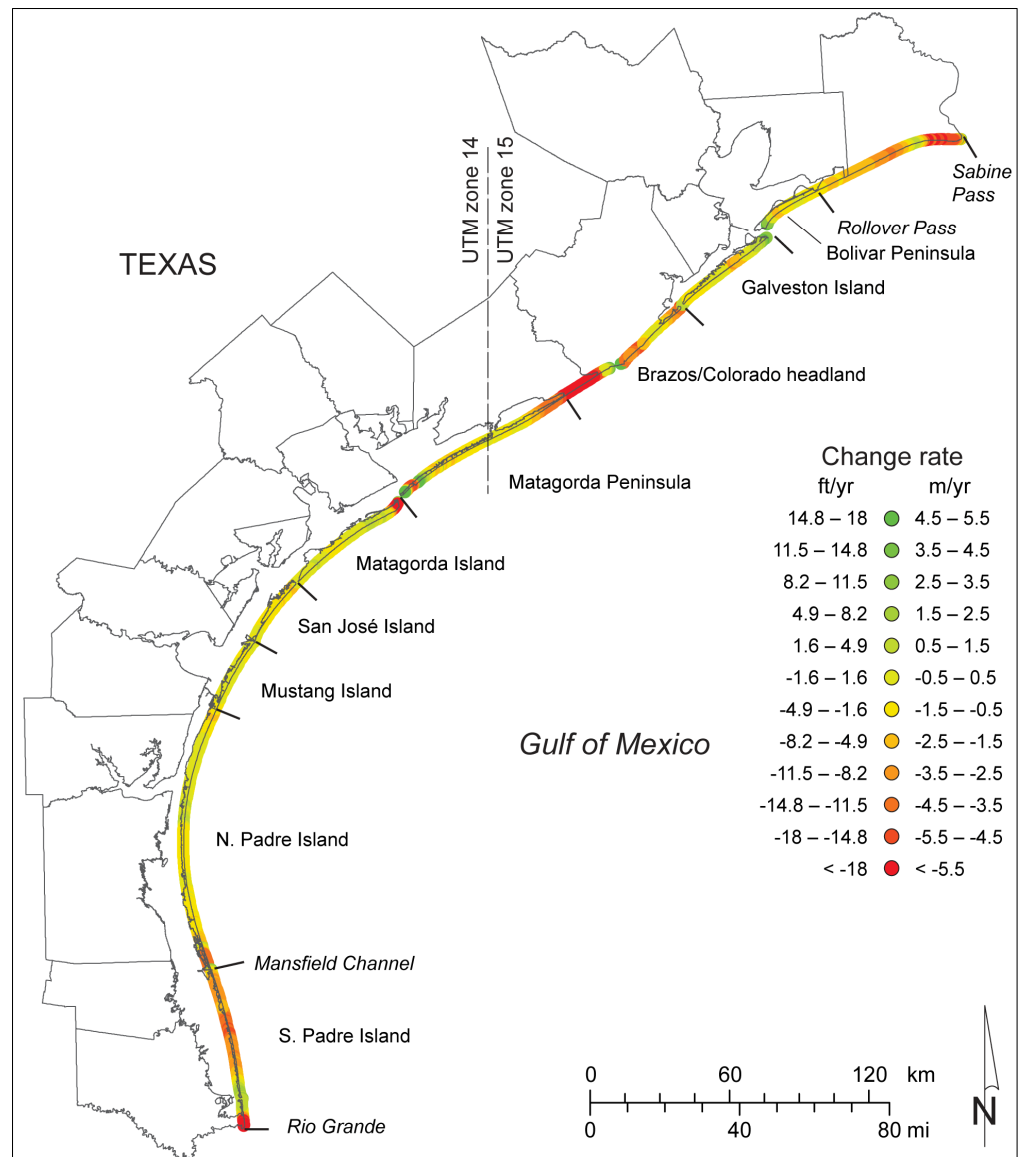
Manuscript received April 8, 2012; revised manuscript received June 19, 2012; manuscript accepted June 19, 2012.

GCAGS Journal, v. 1 (2012), p. 13–26.

that reflects the balance among several important processes, including sea-level rise, land subsidence, sediment influx, littoral drift, and storm frequency and intensity. Because the Texas coast faces ever-increasing developmental pressures as the coastal population swells, an accurate and frequent analysis of shoreline change serves as a planning tool to identify areas of habitat loss, better quantify threats to residential, industrial, and recreational facilities and transportation infrastructure, and help understand the natural and anthropogenic causes of shoreline change.

The latest trends in shoreline change rates are a critical component in understanding the potential impact that sea level, subsi-

Figure 1. Net rates of long-term change for the Texas Gulf of Mexico shoreline between Sabine Pass and the Rio Grande calculated from shoreline positions through 2007. Line segments extending seaward from the shoreline mark boundaries between major coastal segments.



dence, sediment supply, and coastal engineering projects might have on growing coastal population and sensitive coastal environments such as beaches, dunes, and wetlands. Rapidly eroding shorelines threaten coastal habitat and recreational, residential, transportation, and industrial infrastructure and can also increase the vulnerability of coastal communities to tropical storms. Periodic assessments of shoreline position, rates of change, and factors contributing to shoreline change give citizens, organizations, planners, and regulators an indication of expected future change and help determine whether those changes are accelerating, decelerating, or continuing at the same rate as past changes.

Historical change rates of the Texas Gulf shoreline were first determined by the Bureau of Economic Geology (Bureau) in the 1970s and presented in a series of publications covering the 332 mi (535 km) of Gulf shoreline (Morton, 1974, 1975, 1977; Morton and Pieper, 1975a, 1975b, 1976, 1977a, 1977b; Morton et al., 1976). This publication series presented net long-term change rates determined from shoreline positions documented on 1850 to 1882 topographic charts published by the U.S. Coast and Geodetic Survey (Shalowitz, 1964) and aerial photographs acquired between about 1930 and 1975. Rates of change for the entire Gulf shoreline were updated through 1982 based on aerial photographs (Paine and Morton, 1989; Morton and Paine, 1990). Up-

dates for subsets of the Texas Gulf shoreline include the upper coast between Sabine Pass and the Brazos River through 1996 (Morton, 1997) and the Brazos River to Pass Cavallo (Gibeaut et al., 2000) and Mustang and north Padre Island (Gibeaut et al., 2001) segments through 2000 using shoreline positions established using an airborne lidar topographic mapping system. lidar-derived shoreline positions in 2000–2001 were also used as part of a gulf-wide assessment of shoreline change that included the Texas coast (Morton et al., 2004).

This paper discusses results of the 2007 update to the long-term change rates (Paine et al., 2011). The previous rates were calculated from selected shoreline vintages that began in most areas with the 1930s aerial photographs and included Gulf-shoreline-wide aerial photographs acquired through the mid-1990s, ground-based GPS surveys conducted in select areas during the mid-1990s, and coast-wide airborne lidar surveys acquired in 2000. For the 2007 update, we used the boundary between the wet and dry beach, as interpreted from georeferenced aerial photographs taken in September and October 2007, as the most recent shoreline position. We chose 2007 aerial photographs because they are the most recent coast-wide imagery that predated Hurricane Ike, a category 2 hurricane that struck the upper Texas coast in September 2008 and had major impact on

beach morphology and shoreline position. Because the Texas coast undergoes a storm recovery process that can last several years (e.g. Morton and Paine, 1985), the next update of long-term rates will be completed using results of the 2012 airborne lidar survey of the coast, which will allow nearly four years for beach, dune, and vegetation-line recovery from Hurricane Ike.

Relative Sea Level

Changes in sea level relative to the ground surface have long been recognized as a major contributor to shoreline change (e.g. Bruun 1954, 1962, 1988; Cooper and Pilkey, 2004). Rising sea level inundates low-relief coastal lands causing shoreline retreat by submergence, and elevates dynamic coastal processes (currents and waves) that can accelerate shoreline retreat by physical erosion. Changes in relative sea level include both changes in the ocean surface elevation (eustatic sea level) and changes in the elevation of the ground caused by subsidence or uplift. Eustatic sea-level change rates, established by monitoring sea level at long-record tide gauge stations around the world and more recently using satellite altimetry, vary over a range of about 1 to 4 mm/yr. Gutenberg (1941) calculated a eustatic rate of 1.1 mm/yr from tide gauge data. Estimates based on tide gauge data since then have ranged from 1.0 to 1.7 mm/yr (Gornitz et al., 1982; Barnett, 1983; Gornitz and Lebedeff, 1987; Church and White, 2006), although Emery (1980) supported a higher global average of 3.0 mm/yr that is comparable to more recent globally averaged, satellite-based rates. Attempts to remove postglacial isostatic movement and geographical bias from historical tide gauge records resulted in eustatic estimates as high as 2.4 mm/yr (Peltier and Tushingham, 1989). Recent studies that include satellite altimetry data acquired since 1993 indicate that global rates of sea-level rise average 2.8 mm/yr, or 3.1 mm/yr with post-glacial rebound removed (Cazenave and Nerem, 2004). Much of this recent rise is interpreted to arise from thermal expansion of the oceans with a possible contribution from melting of glaciers and polar ice (FitzGerald et al., 2008; Cazenave and Nerem, 2004; Leuliette and Miller, 2009).

In major sedimentary basins such as the northwestern Gulf of Mexico, eustatic sea-level rise is augmented by subsidence. Published rates of relative sea-level rise measured at tide gauges along the Texas coast are higher than eustatic sea-level rates (Swanson and Thurlow, 1973; Lyles et al., 1988; Penland and Ramsey, 1990; Paine, 1991, 1993), ranging from 3.4 to 6.5 mm/yr between 1948 and 1986 for tide gauges at Galveston Pier 21, Rockport, and Port Isabel. These gauges represent single points along the coast and may not be representative of relative sea-level rise along the entire coast. Geodetic releveling data obtained from the National Geodetic Survey at benchmarks along the Texas coast from Galveston Bay to Harlingen show local variation in subsidence rates that would produce average rates of relative sea-level rise ranging from about 2 to more than 20 mm/yr. Despite the wide range, most of the rates fall within the range observed for the long-term Texas tide gauges, suggesting that the gauges are representative regional indicators of relative sea-level rise (Paine, 1991, 1993).

The most recent relative sea-level rise rates from selected Texas tide gauges range from 1.93 to 6.84 mm/yr (Table 1). These rates were calculated by the National Oceanic and Atmospheric Administration through 2006 from periods of record that begin between 1908 (Galveston Pier 21) and 1963 (Port Mansfield). The highest rates (above 5 mm/yr) are calculated for upper and central Texas coast tide gauges at Galveston (Pier 21 and Pleasure Pier), Sabine Pass, and Rockport. The lowest rate (1.93

mm/yr) is calculated for Port Mansfield, which also has the shortest record. The remaining gauges (Port Isabel, north Padre Island, and Freeport) have rates between 3.48 to 4.35 mm/yr.

Galveston Pier 21 has the longest period of record. Long-term rates of sea-level rise calculated from monthly averages of sea level between April 1908 and April 2011 (Fig. 2) are 6.31 mm/yr, similar to the NOAA-calculated rate through 2006. Sea-level rise at this gauge has not been constant. Calculations of average rate of change over a rolling 19-year window (chosen to match the duration of the 19-year National Tidal Datum Epoch and centered on the mid-date) show multiyear oscillations in average rate that range from 1.0 to 13.3 mm/yr (Fig. 2). The most recent rates (since about 1990) are 2.1 to 3.7 mm/yr, among the lowest observed at the gauge, and are similar to satellite altimetry-based eustatic rates for the same period.

Tropical Cyclones

There are numerous examples of the impact that tropical cyclones (tropical storms and hurricanes) have on the Texas Gulf shoreline (e.g. Price, 1956; Hayes, 1967; Morton and Paine, 1985). These include tropical storms and hurricanes that are classified following the Saffir/Simpson hurricane wind scale (Simpson and Riehl, 1981). In general, minimum central pressures decrease as the categories increase, as does pressure- and wind-driven storm surge. Two critical parameters that influence the erosion potential of a tropical cyclone are surge height and surge duration: the longer sea level is elevated above normal during storm passage, the greater the potential for redistribution of sediment eroded from the beach. Beach and dune recovery after storm passage follows several distinct stages and can take years (Morton and Paine, 1985; Morton et al., 1994). The ending date (2007) for this update of long-term shoreline change rates was chosen to predate Hurricane Ike (2008), which was a large Category 2 storm that severely eroded the upper Texas coast. We chose not to include post-Ike shorelines to minimize the transient effect of instantaneous erosion and allow for a recovery period before the next shoreline change-rate update.

Historical accounts and records maintained by the National Oceanic and Atmospheric Administration enumerate 64 hurricanes and 56 tropical storms that have struck the Texas coast since 1850 (Roth, 2010). On average, four hurricanes and four tropical cyclones make landfall in Texas per decade. The longest hurricane-free period in Texas lasted nearly 10 years from October 1989 to August 1999 (Roth, 2010). Parts of the Texas coast for which long-term shoreline change rates had not been determined since the early to mid 1990s fall within this hurricane-free period. Tropical storms such as Frances (1998) had significant impacts on Texas beach and dune systems despite falling short of hurricane strength.

From 1993 through 2010, the period most applicable to this study, 17 tropical cyclones have crossed the Texas coast (Table 2). This includes 11 tropical storms and 6 hurricanes that ranged in strength from Category 1 to Category 3 at landfall. Only 1 hurricane and 4 tropical storms affected Texas during the 1990s. From 2001 to 2010, that number increased to 5 hurricanes and 7 tropical storms. The most severe were Hurricane Bret, a former Category 4 storm that weakened before landfall on Padre Island in August 1999; Hurricane Rita, a Category 5 storm that weakened to Category 3 before landfall in the Sabine Pass area in September 2005; and Hurricane Ike, once a Category 4 storm that heavily eroded upper Texas coast beaches as a very large Category 2 storm associated with an unusually high and long-duration storm surge in September 2008. The most recent storm prior to

Table 1. Long-term rates of relative sea-level rise at select Texas tide gauges through 2006. Data from the National Oceanic and Atmospheric Administration.

Gauge	Beginning year	Period (yr)	Rate (mm/yr)	95% confidence interval (mm/yr)
Sabine Pass	1958	49	5.66	1.07
Galveston Pier 21	1908	99	6.39	0.28
Galveston Pleasure Pier	1957	50	6.84	0.81
Freeport	1954	53	4.35	1.12
Rockport	1948	59	5.16	0.67
Port Mansfield	1963	44	1.93	0.97
Padre Island	1958	49	3.48	0.75
Port Isabel	1944	63	3.64	0.44

the last shoreline position included in this study is Hurricane Rita, which had the greatest impact on the upper Texas coast. Two years elapsed for beach recovery between that storm and the 2007 update.

METHODS

Long-term shoreline change rates were calculated by including the 2007 shoreline into the set of shoreline positions that had been used previously to determine long-term Texas Gulf shoreline change rates presented in the Bureau's shoreline change publication series. Shoreline rates presented in the publications before 2000 were listed as net, or average, rates of change between two end-point dates. More recently, rates have been calculated using linear regression analysis of all included shoreline positions. The 2007 update included both rates (Paine et al., 2011). In most cases, these rates are similar and either rate could be used.

Long-term shoreline change rates were calculated following several steps, including:

- (1) importing 2007 aerial photographs into a geographic information system database;
- (2) checking the georeferencing of 2007 aerial photographs;
- (3) mapping the boundary between the wet beach (generally darker tonal colors) and the dry beach (lighter tones) that represents a shoreline proxy that is consistent with that used for older aerial photographs in previous studies and reasonably corresponds with the 1990s boundaries mapped using ground-based GPS receivers (Morton et al., 1993; Morton, 1997) and with the 2.0 ft (0.6 m) mean sea-level (msl) elevation contour mapped as the shoreline proxy on digital elevation models produced from the 2000 airborne lidar surveys (Gibeaut et al., 2000, 2001);
- (4) selecting the shoreline vintages to use in calculating long-term change rates, which in most cases includes the earliest photograph-derived shoreline from the 1930s Tobin aerial photographs along with geographically extensive coastal photography from the 1950s, 1960s, 1974, 1990s, and 2007;
- (5) creating shore-parallel baselines from which shore-perpendicular transects were cast at 164-ft (50-m) intervals along the shoreline using the GIS-based software Digital Shoreline Analysis System (DSAS; Thieler et al., 2009); and
- (6) calculating long-term rates of change and associated statistics using the transect locations and the selected shorelines within DSAS.

Rates were calculated as linear regression rates and as net (average) rates. Where regression coefficients of determination are relatively high, rates calculated using the linear regression

method reasonably express the long-term movement of the shoreline. Where coefficients are low and fitting errors are high, regression rates may not reasonably reflect the long-term movement of the shoreline. In these cases, net rates that represent the simple average rate of change, calculated by dividing the movement distance by the elapsed time, are preferred.

Shoreline positions on 2007 aerial photographs were mapped by two persons and spot-checked by a third to verify the interpreted position. We also used beach profiles and GPS-mapped shorelines acquired for the Bureau's Texas High School Coastal Monitoring Program (THSCMP) near the dates of photography to verify the wet/dry beach position at long-term monitoring sites on Galveston Island, Follets Island, Matagorda Peninsula, Mustang Island, and Padre Island.

Shorelines used to calculate updated long-term rates included dates chosen for earlier calculations. These may exclude older shorelines in some areas where major engineered structures have impacted shoreline change.

Positional Verification

Georeferencing error is one of the principal sources of potential error in calculations of long-term shoreline change rates (Anders and Byrnes, 1991; Crowell et al., 1991; Moore, 2000). Georeferencing of 2007 aerial photographs was checked through comparison of equivalent natural and constructed features common to 2007 aerial photographs and georeferenced NAIP photographs taken in 2010.

A second check, which addressed the georeferencing of the 2007 photographs and the interpretation of the position of the wet/dry beach boundary, superimposed GPS-based beach profiles and wet/dry beach boundary data acquired in 2007 by the THSCMP and the photo-interpreted 2007 wet/dry beach boundary to be used for change rate calculations. These comparisons, in some cases from ground-based data acquired within a few days of the date of aerial photography, generally showed good agreement (within a few feet) between boundaries interpreted from ground-based data and those interpreted from aerial photographs. Where there is a small discrepancy in the position of the wet/dry beach boundary, the feature mapped on aerial photographs is likely to be more accurately placed than the ground-mapped boundary. Possible sources of error for ground-mapped features include GPS positioning errors and difficulty in identifying tonal changes marking the wet/dry beach boundary.

Comparisons of wet/dry beach position were conducted for THSCMP beach profile sites at Galveston Island State Park, Fol-

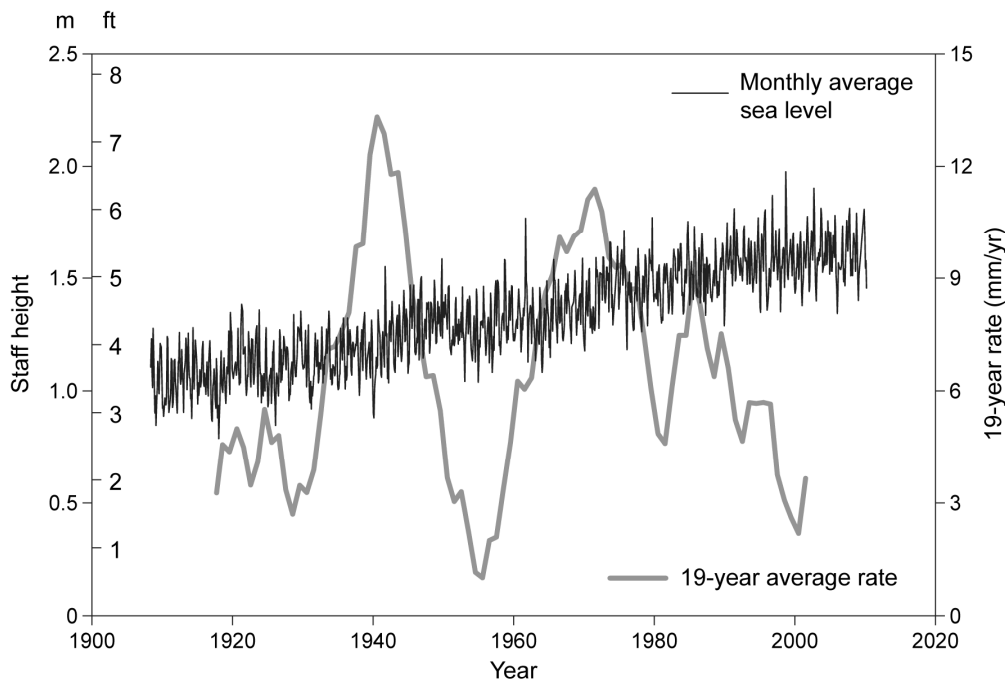


Figure 2. Sea-level trend at Galveston Pleasure Pier, 1908 to 2011. Black line is monthly average sea level. Gray line is the average sea level measured over a 19-yr period (the duration of the National Tidal Datum Epoch) and plotted at the center date of the averaged period. Data from the National Oceanic and Atmospheric Administration.

Table 2. Tropical storms affecting the Texas coast between 1990 and 2010. TS = tropical cyclone; H# = hurricane, where number following H designates numeric strength according to the Saffir/Simpson scale (Simpson and Riehl, 1981). Data from the National Oceanic and Atmospheric Administration and Roth (2010).

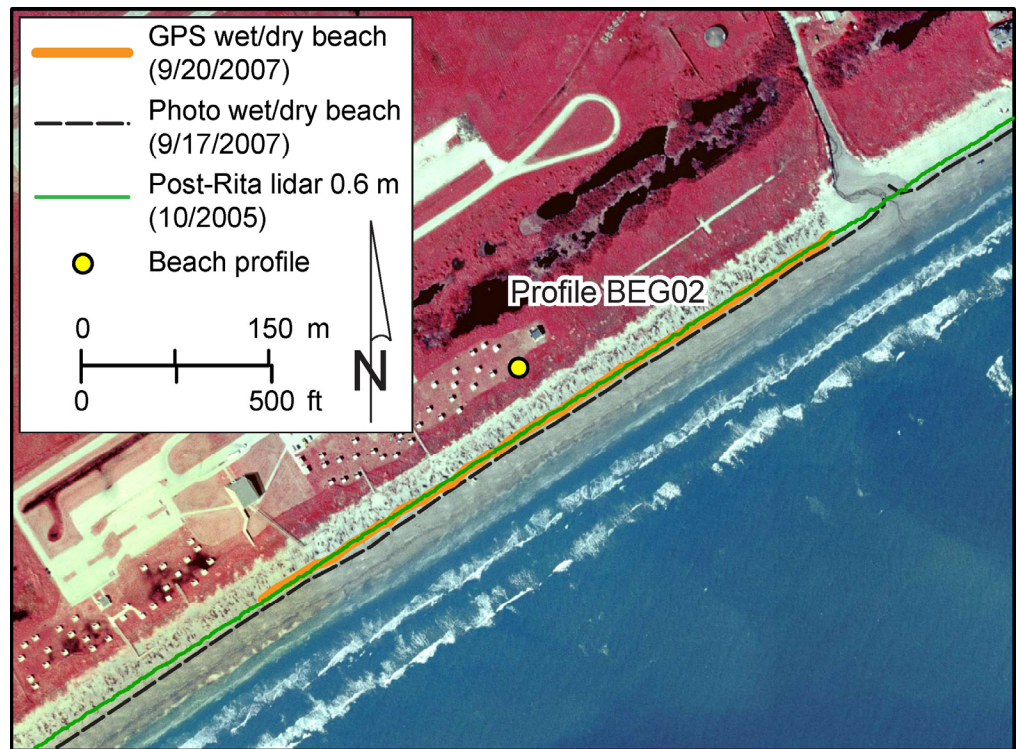
Year	Category	Name	Begin date	End date	Landfall area
1993	TS	Arlene	6/18/1993	6/21/1993	North Padre Island
1995	TS	Dean	7/28/1995	8/2/1995	Freeport
1998	TS	Charley	8/21/1998	8/24/1998	Aransas Pass
1998	TS	Frances	9/8/1998	9/13/1998	Matagorda Island
1999	H4	Bret	8/18/1999	8/25/1999	Padre Island (weakened)
2001	TS	Allison	6/5/2001	6/17/2001	Freeport
2002	TS	Bertha	8/4/2002	8/9/2002	North Padre Island
2002	TS	Fay	9/5/2002	9/8/2002	Matagorda Peninsula
2003	H1	Claudette	7/8/2003	7/17/2003	Matagorda Peninsula
2003	TS	Grace	8/30/2003	9/2/2003	Galveston Island
2005	H5	Rita	9/18/2005	9/26/2005	Sabine Pass (H3 at landfall)
2007	TS	Erin	8/15/2007	8/17/2007	San Jose Island
2007	H1	Humberto	9/12/2007	9/14/2007	Upper Texas coast
2008	H2	Dolly	7/20/2008	7/25/2008	South Padre Island
2008	TS	Edouard	8/3/2008	8/6/2008	Upper Texas coast
2008	H4	Ike	9/1/2008	9/15/2008	Galveston (H2 at landfall)
2010	TS	Hermine	9/5/2010	9/9/2010	Rio Grande area

lets Island, Mustang Island, and South Padre Island. At Galveston Island State Park (Fig. 3), for example, GPS-based wet/dry beach boundary mapped on September 20, 2007, lies generally 13 to 30 ft (4 to 9 m) landward of the same boundary mapped on a 2007 aerial photograph acquired three days earlier (September 17). Analysis of aerial photographs and the beach profile acquired during the ground visit (Fig. 4) suggests that the wet/dry beach boundary mapped using GPS on September 20 was indeed landward of the wet/dry beach boundary mapped on aerial photographs taken on September 17, and that the photograph-based position is consistent with the berm crest identified in the beach profile.

TEXAS GULF SHORELINE CHANGE THROUGH 2007

Rates of long-term Gulf shoreline change, calculated from multiple shoreline positions between the 1930s (mid- to late 1800s in some areas) and 2007 (Fig. 1), averaged 4.1 ft/yr (1.2 m/yr) of retreat (Table 3) for both net rate and linear regression rate calculations. Updated rates were calculated at 11,731 sites along the entire Texas coast spaced at 164 ft (50 m). Net retreat occurred at 9830 sites (84 percent) and advance occurred at 1880 sites (16 percent). The overall rate is lower than the average change rate (retreat at 5.4 ft/yr [1.7 m/yr]) determined from the

Figure 3. Shoreline position comparison at Galveston Island State Park site BEG02. Shorelines include the 2007 wet/dry beach boundary mapped on aerial photographs taken on 9/17/2007, the wet/dry beach boundary mapped on 9/20/2007 by THSCMP students and staff using ground GPS, and the 2.0 ft (0.6 m) msl shoreline proxy extracted from airborne lidar data acquired after Hurricane Rita in October 2005.



previous update (through the mid 1990s to 2000), but the previous rates exclude central and lower coast segments on San José, Matagorda, and central Padre Islands that have generally low rates of change (slow advance to slow retreat). Shorelines along the upper Texas coast (from the mouth of the Colorado River to Sabine Pass) generally retreated at greater rates than those on the central and lower coast. Averages of change rates were retreat at 5.3 ft/yr (1.6 m/yr) for the upper coast and retreat at 3.3 ft/yr (1.0 m/yr) for the central and lower coast (Table 3).

Notable extensive areas of relatively high long-term retreat rates include (1) the High Island to Sabine Pass area, (2) an area on Galveston Island west of the Galveston seawall, (3) the combined deltaic headland of the Brazos and Colorado rivers, (4) Matagorda Peninsula west of the Colorado River, (5) San José Island, and (6) the northern part and most of the southern half of Padre Island. Areas of general net shoreline advance are found (1) on the upper coast near the Sabine Pass and Bolivar Roads jetties, (2) at the western tip of Galveston Island, (3) on the Brazos/Colorado deltaic headland near the mouth of the Brazos River, (4) toward the western end of Matagorda Peninsula, (5) on the central Texas coast along much of Matagorda Island and near Aransas Pass, and (6) on Padre Island near Baffin Bay and the southern end of the island.

Closely spaced measurement sites allow estimates of land loss to be made (Table 3). The annual rate of land loss along the Texas Gulf shoreline, updated through 2007, is 180 ac/yr (73 ha/yr). Total Texas Gulf shoreline land loss from 1930 through 2007 is 13,890 ac (5621 ha).

Upper Texas Coast (Sabine Pass to San Luis Pass)

The upper Texas coast extends about 88 mi (141 km) from Sabine Pass at the Texas-Louisiana border to San Luis Pass at the southwestern end of Galveston Island (Figs. 1 and 5). Major natural geomorphic features and shoreline types are (1) the generally shore-parallel beach ridges and intervening swales in the

Sabine Pass area, (2) thin, discontinuous sandy beaches that veneer the retreating low, muddy marsh deposits between High Island and Sea Rim State Park, (3) the broad, sandy beach and dune system on Bolivar Peninsula, and (4) the sandy barrier island system at Galveston Island. Major engineered structures that have affected the sediment budget and shoreline change rates include major jetty and dredged channel systems at Sabine Pass and Bolivar Roads, a shallow (5 ft [1.5 m]) dredged channel across Bolivar Peninsula at Rollover Pass, and the Galveston seawall (shore-parallel wall) and groin field (shore-normal structures that trap littoral sediment) on the eastern third of Galveston Island. At Sabine Pass, the south jetty extends about 2.5 mi (4 km) from the shoreline and protects a channel maintained at a depth of 40 ft (12 m). The Sabine Pass jetties and channel isolate the upper Texas coast from potential easterly sources of longshore sediment. The Bolivar Roads channel, maintained at a depth of 45 ft (14 m), is protected by jetties that extend 4.7 mi (7.6 km) (north jetty) and 2.4 mi (3.9 km) (south jetty) from the shoreline. The jetties and channel serve to compartmentalize the upper Texas coast by blocking longshore transport of sand between Bolivar Peninsula and Galveston Island.

Nearly 88 percent of the measurement sites on the upper Texas coast (2468 of 2810) showed net shoreline retreat through 2007. Net rates at individual measuring points on the upper Texas coast range from retreat at 27.9 ft/yr (8.5 m/yr) to advance at 36.7 ft/yr (11.2 m/yr). Net land loss since 1930 is estimated to be 3200 ac (1295 ha) between Sabine Pass and High Island, 20 ac (8 ha) on Bolivar Peninsula west of Rollover Pass, and 213 ac (86 ha) on Galveston Island. Long segments of retreating shorelines extend from near Sabine Pass to High Island, between High Island and Gilchrist, on the western part of Bolivar Peninsula southwest of Crystal Beach, on Galveston Island along a 6.2-mi (10-km) shoreline segment west of the seawall, and on the western end of Galveston Island (Fig. 5). Areas of net advance are limited, but include a short shoreline segment adjacent to the south jetty at Sabine Pass, a 1.9-mi (3-km)-long segment near

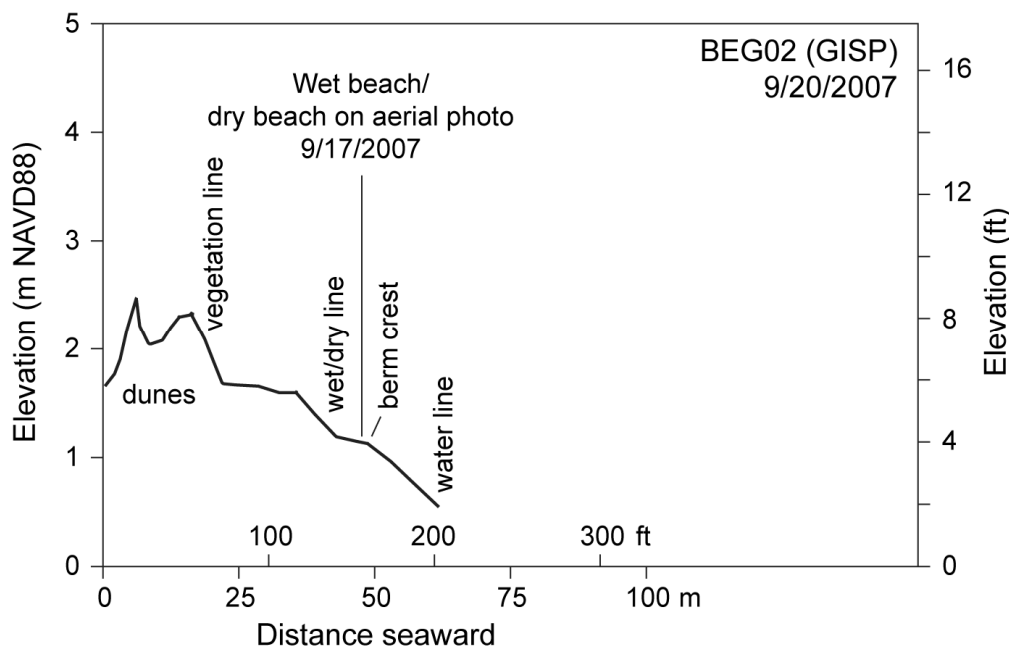


Figure 4. Beach profile at Galveston Island State Park site BEG02 (Fig. 3) with superimposed wet/dry beach boundary mapped on 2007 aerial photographs. Profile acquired on 9/20/2007 by THSCMP students and staff.

Sea Rim State Park, shoreline segments a few miles long adjacent to the north and south jetties at Bolivar Roads, and a short segment at the southwestern end of Galveston Island adjacent to San Luis Pass.

Follets Island, Brazos and Colorado Headland, and Matagorda Peninsula

Between San Luis Pass and Pass Cavallo lies the headland of the Brazos and Colorado river deltas and flanking barrier peninsulas Follets Island and Matagorda Peninsula (Figs. 1 and 6). This segment includes about 89 mi (143 km) of Gulf of Mexico shoreline. Major geologic features are: (1) the combined Brazos and Colorado deltaic headland, consisting of semi-consolidated, muddy and sandy sediments deposited by the Brazos and Colorado rivers and overlain by a discontinuous, thin veneer of sandy beach deposits; (2) a narrow, sandy barrier peninsula extending northeastward from the Brazos headland toward San Luis Pass (Follets Island); and (3) a narrow, sandy barrier peninsula extending southwestward from the Colorado headland toward Pass Cavallo (Matagorda Peninsula). Sediments eroded by waves at the headland contribute sand to the flanking barrier peninsulas. In addition, the Brazos and Colorado rivers historically brought sediment to the coast from their large drainage basins. The drainage basin of the Brazos River covers more than 45,300 mi² (117,300 km²) in Texas and eastern New Mexico (Dougherty, 1980), but its capacity for carrying sediment to the coast during major floods has been reduced by completion of several dams and reservoirs between 1941 and 1969 (Possum Kingdom, Whitney, Granbury, and DeCordova Bend). The drainage basin of the Colorado is nearly as large (more than 41,600 mi², or 107,700 km²; Dougherty, 1980), but its sediment-carrying capacity has also been reduced by nine dams completed in the upper and central basins between 1937 and 1990 (Buchanan, Inks, Tom Miller, Mansfield, Wirtz, Starcke, Thomas, Lee, and Ivie) and diversion into Matagorda Bay. This segment of Gulf shoreline has been compartmentalized by jetties and dredged channels. Between Quintana and Surfside Beach, the Freeport jetties extend about

3300 ft (1000 m) from the shoreline to reduce dredging needs of the Freeport Ship Channel, which has been dredged to a depth of 45 ft (14 m). On Matagorda Peninsula, shorter jetties extend 460 to 790 ft (140 to 240 m) seaward from the mouth of the Colorado River. The Matagorda Ship Channel, maintained at a dredged depth of 36 ft (11 m) near the southwestern end of Matagorda Peninsula, is flanked by jetties that extend 2900 ft (880 m) (north jetty) and 5250 ft (1600 m) (south jetty) into the Gulf.

There was net shoreline retreat at 2417 of 2837 (85 percent) measurement sites between San Luis Pass and Pass Cavallo. Net rates of change through 2007 ranged from retreat at 33.5 ft/yr (10.2 m/yr) to advance at 84.0 ft/yr (25.6 m/y). Notable areas of long-term shoreline retreat include (1) Follets Island, (2) the Brazos headland between Surfside Beach and the mouth of the Brazos River and from Sargent Beach to the San Bernard National Wildlife Refuge, and (3) a segment of Matagorda Peninsula southwest of the Matagorda Ship Channel (Fig. 6). Shorelines having net advance are limited to short segments on Matagorda Peninsula, including a 2-mi- (3-km)-long segment northeast of the mouth of the Colorado River, a 3.4-mi (5.5-km)-long segment adjacent to the north jetty at the Matagorda Ship Channel, and a 1.2-mi (2-km)-long segment at the southwestern tip of the peninsula. When integrated over the entire measurement period since 1930 (Table 3), the estimated loss of land along the Brazos/Colorado headland and flanking peninsulas is 4160 ac (1684 ha).

Central Texas Coast (Matagorda, San José, and Mustang Islands)

Gulf shorelines along the central Texas coast between Pass Cavallo and Packery Channel include those on three sandy barrier islands: Matagorda Island, San José Island, and Mustang Island (Figs. 1 and 7). These sand-rich islands are characterized by broad, sandy beaches and dune systems that reflect the position of the islands within a longshore current convergence zone between the Brazos/Colorado and Rio Grande fluvial/deltaic headlands. The natural boundaries between these three islands are Cedar Bayou, a tidal inlet between Matagorda and San José

Table 3. Historical net shoreline change rates and land loss through 2007 for the Texas Gulf shoreline calculated for all measurement points along the coast and within shoreline segments (Fig. 1). Negative values indicate shoreline retreat; positive values indicate shoreline advance. Land loss rates and areas are normalized to the 1930 to 2007 period.

Area	No.	Net rate (ft/yr)	Std. Dev. (ft/yr)	Range (ft/yr)	Land loss rate (ac/yr)	Land loss (ac)
All Texas sites	11,731	-4.1	9.8	-56.2 to 84.0	180	13,890
Upper coast (Sabine Pass to Colorado River)	4797	-5.3	12.0	-33.4 to 68.8	96	7358
Lower coast (Colorado River to Rio Grande)	6934	-3.3	7.9	-56.2 to 84.0	85	6532
Sabine Pass to High Island	1335	-8.3	6.3	-27.7 to 31.0	41.6	3200
Bolivar Peninsula	547	-0.1	7.8	-5.5 to 36.6	0.2	18
Galveston Island	928	-0.8	5.9	-10.0 to 21.6	2.8	213
Brazos/Colorado headland	1250	-6.9	19.9	-33.4 to 68.8	32.4	2497
Matagorda Peninsula	1589	-3.6	10.2	-28.5 to 84.0	21.6	1666
Matagorda Island	1120	-2.7	13.0	-56.2 to 58.0	11.5	888
San Jose Island	632	-3.2	1.7	-6.5 to 0.9	7.6	589
Mustang Island	575	-0.7	1.4	-4.4 to 1.9	1.5	113
N. Padre Island	2398	-2.5	3.3	-14.6 to 5.4	22.9	1762
S. Padre Island	1357	-7.5	6.4	-24.5 to 10.6	38.3	2945

islands, and Aransas Pass, a tidal inlet between San José and Mustang Islands. No rivers directly reach the Gulf within this segment.

Engineered structures that have compartmentalized the near-shore system are (1) the Matagorda Ship Channel and jetties that restrict sediment transport to Matagorda Island from the northeast, and (2) the jetties at Aransas Pass, which protect the dredged, 47-ft (14-m) deep Corpus Christi Ship Channel. These jetties extend 3600 to 3950 ft (1100 to 1200 m) gulfward from the shoreline, interrupting longshore sand exchange between Mustang and San José Islands. Smaller structures with possible local effects include the closed Fish Pass on Mustang Island, where the former dredged channel is filled but short jetties that extend about 500 ft (150 m) from the shoreline remain; and Packery Channel, a newly constructed shallow channel between Mustang and Padre islands that has been dredged to a nominal depth of 10 ft (3 m) and is protected by jetties that reach 1000 ft (300 m) (north jetty) and 1200 ft (365 m) (south jetty) seaward of the Gulf shoreline.

Long-term Gulf shoreline change rates within this segment of the Texas coast were calculated at 2,419 sites over a distance of 75 mi (121 km) between Pass Cavallo and the southern end of Mustang Island (Fig. 7). Net shoreline change rates calculated through 2007 averaged retreat at 2.7 ft/yr (0.8 m/yr) for Matagorda Island, retreat at 3.2 ft/yr (1.0 m/yr) for San José Island, and retreat at 0.9 ft/yr (0.3 m/yr) for Mustang Island. Estimated total land loss since 1930 is 887 ac (359 ha) on Matagorda Island, 588 ac (238 ha) on San José Island, and 114 ac (46 ha) on Mustang Island (Table 3).

The majority of measuring sites underwent net shoreline retreat (1872 of 2419; 77 percent). Net rates at individual sites ranged from retreat at 56 ft/yr (17 m/yr) to advance at 59 ft/yr (18 m/yr). Nearly half the Gulf shoreline of Matagorda Island has advanced since 1937, albeit at low rates except along a short segment where the island has migrated toward Pass Cavallo at its northeastern end. Sites along short shoreline segments near the north and south jetties of the Corpus Christi Ship Channel re-

corded minor net shoreline advance. Highest rates of net retreat (more than 10 ft/yr [3 m/yr]) were measured along a 3.7-mi (6-km)-long segment of Matagorda Island near Pass Cavallo. Net retreat rates greater than 3 ft/yr (1 m/yr) were measured along much of San José Island (as much as 6.5 ft/yr [2 m/yr]), along a 3-mi (5-km)-long segment in the middle part of Mustang Island where retreat rates were as high as 4.1 ft/yr (1.2 m/yr), and along the southern tip of Mustang Island where net retreat averaged as much as 4.4 ft/yr (1.4 m/yr).

Lower Coast (Padre Island)

The lower coast segment encompasses 114 mi (183 km) of Gulf shoreline (Figs. 1 and 8), where shoreline change rates were calculated at 3663 sites. The principal geomorphic feature in this area is Padre Island, which broadens from a narrow peninsula at its southern end at Brazos Santiago Pass to a broad, sandy barrier island having a well-developed dune system throughout most of its length. The Rio Grande enters the Gulf of Mexico within this segment and has created a large fluvial/deltaic headland that forms the southern boundary of a regional longshore current cell that is bounded on the north by the Brazos/Colorado headland. The Rio Grande has a large drainage basin (more than 176,300 mi² [456,600 km²]) (Dougherty, 1980) that extends into Mexico, New Mexico, and Colorado, but dams constructed on the middle and lower parts of the basin in 1954 (Falcon) and 1969 (Amistad), combined with extensive irrigation use of Rio Grande water on the coastal plain, has reduced the amount of sediment delivered to the coast.

Most of Padre Island is undeveloped, except for intensive development at its northern extremity (Corpus Christi) and at the southern tip of the island (the city of South Padre Island). Engineered structures that have affected shoreline position include (1) the jetties and associated ship channel at Brazos Santiago Pass, where the 44-ft (13-m) deep channel is flanked by jetties that reach 2850 ft (870 m) (north jetty) and 1600 ft (490 m) (south jetty) into the Gulf; and (2) the shallower Port Mansfield Channel

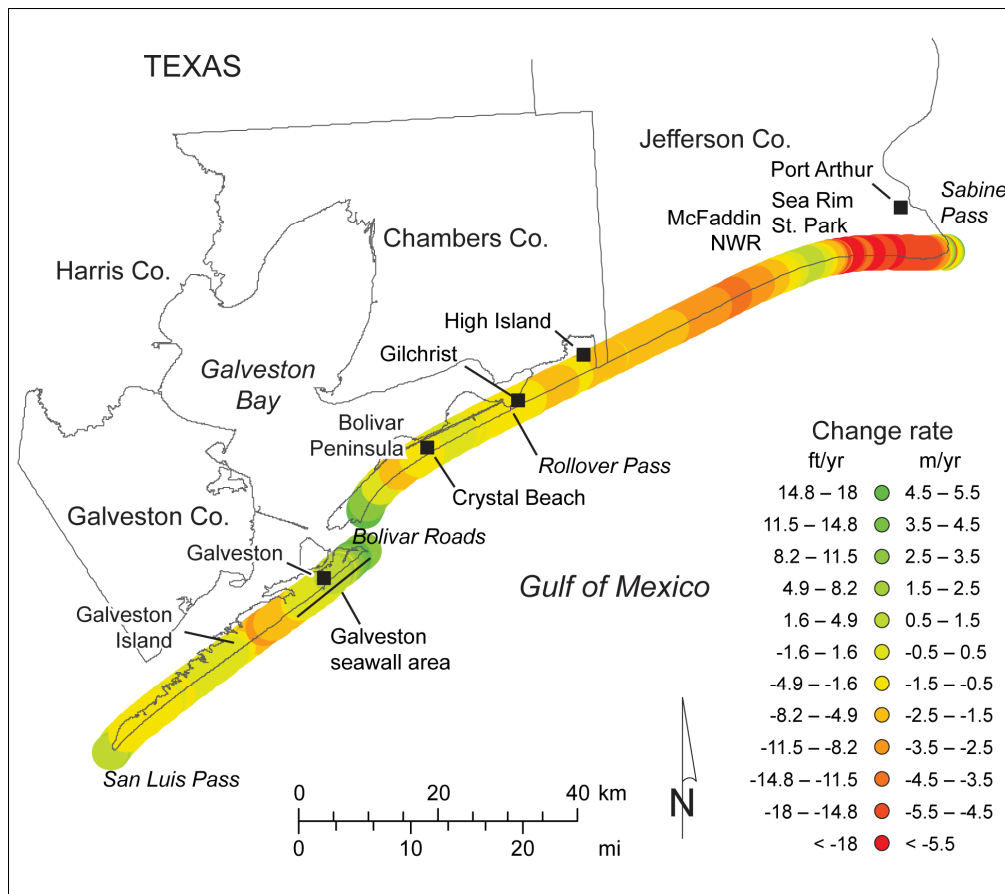


Figure 5. Net rates of long-term change for the upper Texas Gulf shoreline between Sabine Pass and San Luis Pass (Sabine Pass to Rollover Pass, Bolivar Peninsula, and Galveston Island) calculated from shoreline positions through 2007.

and its 2030 ft (620 m) (north) and 460 ft (140 m) (south) jetties that protect the 15-ft (5-m) deep channel.

Net shoreline change rates average retreat at 2.5 ft/yr (0.8 m/yr) on northern Padre Island and 7.5 ft/yr (2.3 m/yr) on southern Padre Island (Fig. 8 and Table 3). Estimated net land loss since 1930 is 1762 ac (713 ha) for northern Padre Island and 2945 ac (1192 ha) for southern Padre Island.

Despite the location of much of Padre Island in a longshore drift convergence zone, the shoreline retreated at 3073 of 3663 measurement sites (84 percent). Net change rates at individual sites ranged from advance at 10.5 ft/yr (3.2 m/yr) to retreat at 24.6 ft/yr (7.5 m/yr). Net advancing shorelines include two nearly 3-mi (5-km)-long segments adjacent to the north and south jetties at Brazos Santiago Pass, a 9-mi (15-km)-long segment in the Little Shell Beach area on Padre Island National Seashore near Baffin Bay, and a 3-mi (5-km)-long segment on the northern part of Padre Island National Seashore (Fig. 8). Highest rates of net retreat (greater than 10 ft/yr [3 m/yr]) were measured along a 5-mi (8-km)-long segment north of the Mansfield Channel jetties, along a 14-mi (23-km)-long segment in northern Cameron County (Fig. 8), and along a 2-mi (3-km)-long segment south of Brazos Santiago Pass at Boca Chica.

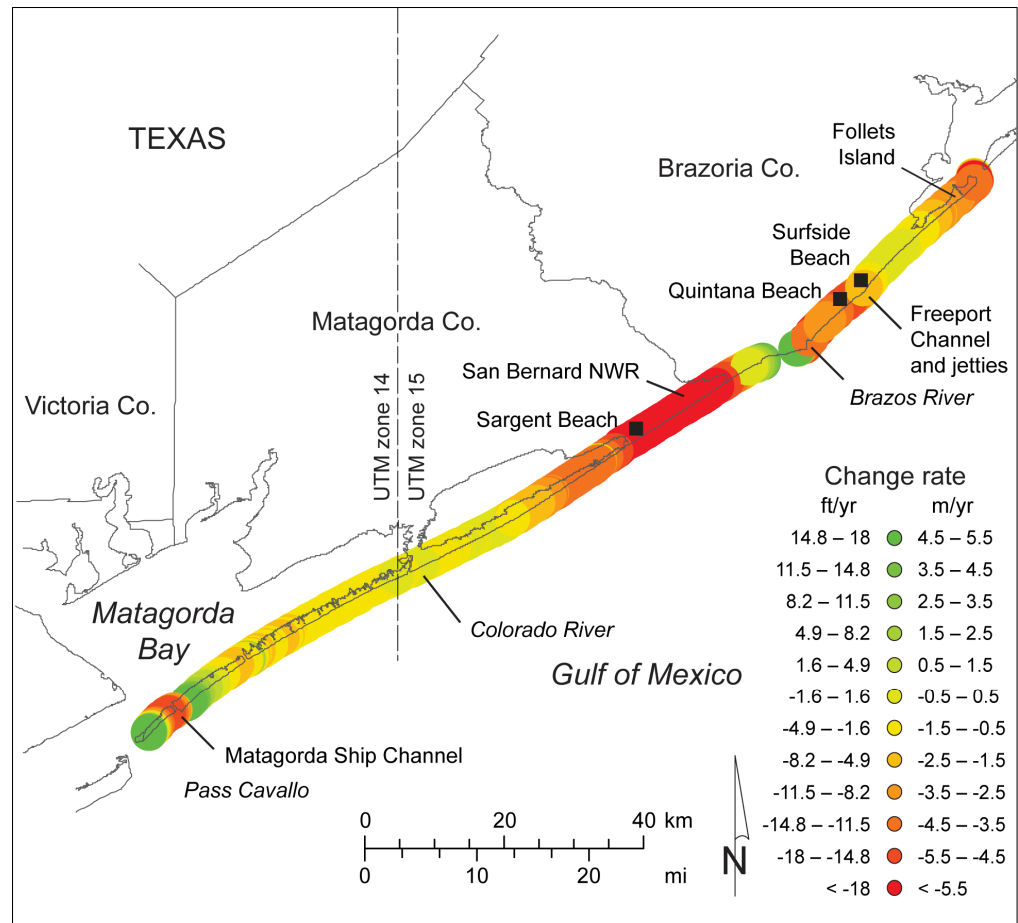
LATE PLEISTOCENE TO MID-HOLOCENE CONTEXT

Estimates of shoreline change rates over geologic intervals can provide a useful context for historical rates documented from maps, aerial photographs, beach surveys, and airborne surveys acquired over many decades. One simple approach to estimating

net change rates since the end of the last glacial maximum at about 20 ka, when sea level was several hundred feet lower than it is today, is to use shelf bathymetric contours (Fig. 9) as a proxy for shoreline position at past sea-level elevations. Rates of post-glacial shoreline change can be estimated by measuring the shore-normal distance between selected bathymetric contours on the Texas shelf and the present shoreline position and dividing by the elapsed time since sea level was at those elevations (Table 4). Subsidence, which is likely to vary spatially and temporally, is a substantial source of error for this approach. Nevertheless, the impact of subsidence on the rates is partly offset by the fact that the Gulf of Mexico sea-level curves (Balsillie and Donoghue, 2004, 2009; Milliken et al., 2008) have also been constructed without correcting for the effects of subsidence. Holocene shelf sedimentation is another source of error that can be significant (particularly within major incised valleys on the inner continental shelf), but is presumed to be minimal in the context of generalized bathymetric contours extending along the entire continental shelf.

This order-of-magnitude approach yields estimated net retreat rates between 16 ka and the present that range from about 8 to 44 ft/yr (2 to 13 m/yr, Table 4), reflecting rapid sea-level rise rates (Balsillie and Donoghue, 2004, 2009; Milliken et al., 2008) and rapid general shoreline retreat during the late Pleistocene and early Holocene. Higher long-term rates are calculated for the upper coast than for the lower coast. Beginning at about 10 ka, net rates generally decrease along the entire coast as the beginning shoreline position date becomes younger; nevertheless, the trend of higher retreat rates on the upper coast and lower rates on the lower coast is consistent for each period. From 11 ka to pre-

Figure 6. Net rates of long-term change for the Texas Gulf shoreline along Follets Island, the Brazos and Colorado headland, and Matagorda Peninsula between San Luis Pass and Pass Cavallo.



sent, for example, estimated retreat rates ranged from 9 ft/yr (3 m/yr) along the South Padre Island transect to 40 ft/yr (12 m/yr) along the Sabine Pass transect. From 8 ka to present, net rates decreased to 0.6 ft/yr (0.2 m/yr) on Padre Island and 5 ft/yr (1.7 m/yr) at Sabine Pass. Published sea-level curves for the northern Gulf of Mexico (Balsillie and Donoghue, 2004, 2009; Milliken et al., 2008) show a reduction in rates of sea-level rise that began between about 8 and 10 ka that coincides with lower estimated rates of postglacial shoreline retreat.

Shoreline change rates can also be estimated for discrete intervals within the general postglacial sea-level rise by comparing past successive sea-level positions and generalized bathymetric contours as a shoreline proxy (Table 4). These data show that estimated net retreat rates were very high before 8 ka, ranging from 8 to 181 ft/yr (2 to 55 m/yr) depending on the interval and location (upper coast rates are generally significantly higher than middle- and lower-coast rates). The highest rates of shoreline retreat occurred between 11 ka and 10 ka, when rates ranged between 60 ft/yr (18 m/yr) along the South Padre Island transect and 181 ft/yr (55 m/yr) along the Sabine Pass transect. Rates between 8 and 7 ka lowered significantly to 2 to 21 ft/yr (0.7 to 6.3 m/yr), as did those since 7 ka (0.4 to 3.3 ft/yr [0.1 to 1 m/yr]). In this context, historical retreat rates averaging 5.3 ft/yr on the upper Texas coast and 3.3 ft/yr on the lower Texas coast (calculated from decades-long datasets derived from aerial photographs and shoreline surveys) are significantly lower than late Pleistocene to early Holocene retreat estimates during times of rapid postglacial sea-level rise and are similar to retreat rates estimated since the mid-Holocene when sea-level rise rates decreased.

CONCLUSIONS

Long-term rates of Texas Gulf shoreline change have been updated through 2007 from a series of shoreline positions that include those from 1800s topographic charts, aerial photographs from the 1930s through 2007, ground GPS surveys from the mid-1990s, and an airborne lidar survey conducted in 2000.

From 1993 to 2007, the period that would most influence changes in rates between this update and the previous one (through the mid-1990s to 2000), tropical cyclone frequency was near the historical incidence of 0.8 cyclones per year. There were nine tropical storms and four hurricanes that made landfall on the Texas coast, including five on the upper coast, five on the central coast, and three on the lower coast. Relative sea-level rise rates at Galveston for the period were at the low end of historically observed rates (2.1 to 3.7 mm/yr) and were near global (eustatic) rates.

Change rates calculated at 11,731 sites spaced at 164-ft (50-m) intervals averaged net retreat at 4.1 ft/yr (1.2 m/yr) through 2007. Average change rates were more recessional on the upper Texas coast (5.3 ft/yr [1.6 m/yr]) than they were on the central and lower coast (3.3 ft/yr [1.0 m/yr]). Annual rates of land loss along the Texas Gulf shoreline average 180 ac/yr (73 ha/yr). Total estimated land loss since 1930, when aerial photography-based shoreline monitoring became possible, is estimated to be 13,890 ac (5620 ha). Historical shoreline retreat rates calculated from shoreline positions determined from aerial photographs and ground and airborne surveys, when compared to longer-term rates estimated from bathymetric contour shoreline proxies and past sea-level positions, are significantly lower than late Pleisto-

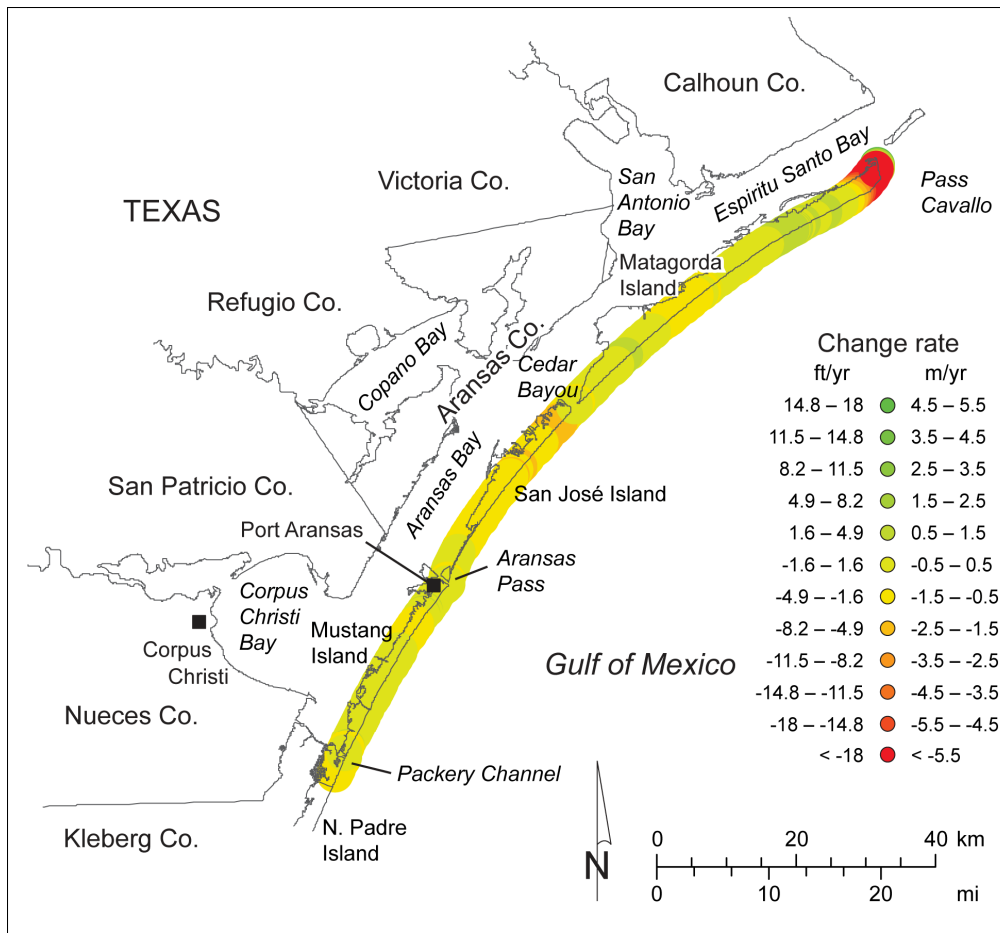


Figure 7. Net rates of long-term change for the central Texas Gulf shoreline between Pass Cavallo and the Packery Channel area (Matagorda Island, San José Island, and Mustang Island) calculated from shoreline positions through 2007.

cene to early Holocene retreat rates of 8 to 181 ft/yr (2.5 to 55.2 m/yr) but are similar to retreat rates of 0.4 to 5.4 ft/yr (0.1 to 1.7 m/yr) estimated since the mid-Holocene.

ACKNOWLEDGMENTS

This project was supported by grant no. 10-041-000-3737 from the General Land Office of Texas to the Bureau of Economic Geology, The University of Texas at Austin. Jeffrey G. Paine served as the principal investigator. The project was funded under a Coastal Management Program (Cycle 14) grant made available to the State of Texas by the U.S. Department of Commerce, National Oceanic and Atmospheric Administration pursuant to the Federal Coastal Zone Management Act of 1972. Supporting funds from the State of Texas were provided through the Coastal Erosion Planning and Response Act (CEPRA) program administered by the General Land Office. Technical reviews by Ray Newby, Dan'l Lewis, and James Gibeaut helped improve the manuscript. Publication authorized by the Director, Bureau of Economic Geology, Jackson School of Geosciences, University of Texas at Austin.

REFERENCES CITED

Anders, F. J., and M. R. Byrnes, 1991, Accuracy of shoreline change rates as determined from maps and aerial photographs: *Shore and Beach*, v. 59, p. 17–26.

Balsillie, J. H., and J. F. Donoghue, 2009, Chapter 4: Northern Gulf of Mexico sea-level history for the past 20,000 years: *in* C. W. Holmes, ed., *The Gulf of Mexico, its origin, waters, biota and*

Human impacts: *Geology: Harte Research Institute for Gulf of Mexico Studies, Corpus Christi, Texas*, v. 1, p. 53–69.

Balsillie, J. H., and J. F. Donoghue, 2004, High resolution sea-level history for the Gulf of Mexico since the last glacial maximum, Florida Geological Survey Report of Investigations 103, Tallahassee, Florida, p. 53–69.

Barnett, T. P., 1983, Global sea level: Estimating and explaining apparent changes: *in* O. T. Magoon, and H. Converse, eds., *Coastal Zone '83, Proceedings of the Third Symposium on Coastal and Ocean Management*, v. 3, San Diego, California, p. 2777–2783.

Bruun, P., 1954, Coastal erosion and development of beach profiles: U. S. Army Corps of Engineers, Beach Erosion Board Technical Memorandum 44, Washington, DC, 82 p.

Bruun, P., 1962, Sea-level rise as a cause of shore erosion: *Journal of the Waterways and Harbors Division*, v. 88, p. 117–130.

Bruun, P., 1988, The Bruun rule of erosion by sea-level rise: A discussion of large-scale two- and three-dimensional usages: *Journal of Coastal Research*, v. 4, p. 627–648.

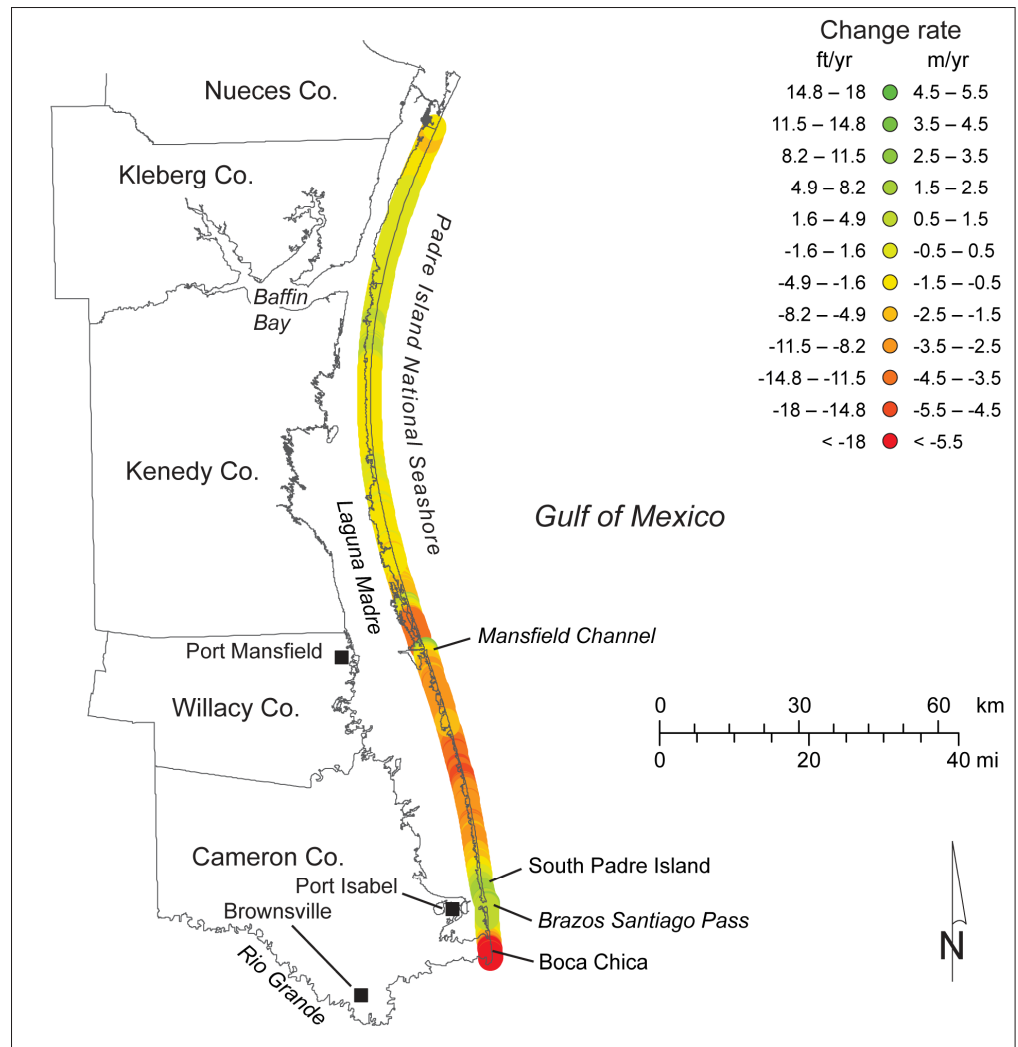
Cazenave, A., and R. S. Nerem, 2004, Present-day sea level change: Observations and causes: *Reviews of Geophysics*, v. 42, RG3001, doi:10.1029/2003RG000139, 20 p.

Church, J. A., and N. J. White, 2006, A 20th century acceleration in global sea-level rise: *Geophysical Research Letters*, v. 33, L01602, doi:10.1029/2005GL024826.

Cooper, J. A. G., and O. H. Pilkey, 2004, Sea-level rise and shoreline retreat: Time to abandon the Bruun Rule: *Global and Planetary Change*, v. 43, p. 157–171.

Crowell, M., S. P. Leatherman, and M. K. Buckley, 1991, Historical shoreline change: Error analysis and mapping accuracy: *Journal of Coastal Research*, v. 7, p. 839–852.

Figure 8. Net rates of long-term change for the lower Texas Gulf shoreline along Padre Island calculated from shoreline positions through 2007.



- Dougherty, J. P., 1980, Streamflow and reservoir-content records in Texas: Compilation report January 1889 through December 1975: Texas Department of Water Resources Report 244, v. 2, Austin, 308 p.
- Emery, K. O., 1980, Relative sea levels from tide-gauge records: Proceedings of the National Academy of Sciences, United States of America, v. 77, p. 6968–6972.
- FitzGerald, D. M., M. S. Fenster, B. A. Argow, and I. V. Buynevich, 2008, Coastal impacts due to sea-level rise: Annual Review of Earth and Planetary Sciences, v. 36, p. 601–647.
- Gibeaut, J. C., T. Hepner, R. Waldinger, J. Andrews, R. Gutierrez, T. A. Tremblay, and R. Smyth, 2001, Changes in gulf shoreline position, Mustang and north Padre islands, Texas: Report by the Texas Bureau of Economic Geology for the Texas Coastal Coordination Council and the General Land Office under Contract 00–002r, Austin, 29 p.
- Gibeaut, J. C., W. A. White, T. Hepner, R. Gutierrez, T. A. Tremblay, R. A. Smyth, and J. Andrews, 2000, Texas shoreline change project: Gulf of Mexico shoreline change from the Brazos river to Pass Cavallo: Report by the Texas Bureau of Economic Geology for the Texas Coastal Coordination Council and the General Land Office under Contract NA870Z0251, Austin, 32 p.
- Gornitz, V., S. Lebedeff, and J. Hansen, 1982, Global sea level trend in the past century: Science, v. 215, p. 1611–1614.
- Gornitz, V., and S. Lebedeff, 1987, Global sea-level changes during the past century, in D. Nummedal, O. H. Pilkey, and J. D. Howard, eds., Sea level fluctuation and coastal evolution: Society of Economic Paleontologists and Mineralogists Special Publication 41, Tulsa, Oklahoma, p. 3–16.
- Gutenberg, B., 1941, Changes in sea level, postglacial uplift, and mobility of the earth's interior: Geological Society of America Bulletin, v. 52, p. 721–772.
- Hayes, M. O., 1967, Hurricanes as geological agents: Case studies of hurricanes Carla, 1961, and Cindy, 1963: Texas Bureau of Economic Geology Report of Investigations 61, Austin, 54 p.
- Holcombe, T. L., and C. Arias, 2009, Bathymetry of Texas-Louisiana continental shelf and coastal regions compatible with geographic information systems – bathymetry (GIS data set, version 2): Department of Oceanography, Texas A&M University, College Station, digital dataset.
- Leuliette, E. W., and L. Miller, 2009, Closing the sea level rise budget with altimetry, Argo, and GRACE: Geophysical Research Letters, v. 36, L04608, doi:10.1029/2008GL036010.
- Lyles, S. D., L. E. Hickman, Jr., and H. A. Debaugh, Jr., 1988, Sea level variations for the United States, 1855–1986: National Ocean Service, Rockville, Maryland, 182 p.
- Milliken, K. T., J. B. Anderson, and A. B. Rodriguez, 2008, A new composite Holocene sea-level curve for the northern Gulf of Mexico, in J. B. Anderson, and A. B. Rodriguez, eds., Response of upper Gulf Coast estuaries to Holocene climate change and sea-level rise: Geological Society of America Special Paper 443, Boulder, Colorado, p. 1–11, doi:10.1130/2008.2443(01).
- Moore, L. J., 2000, Shoreline mapping techniques: Journal of

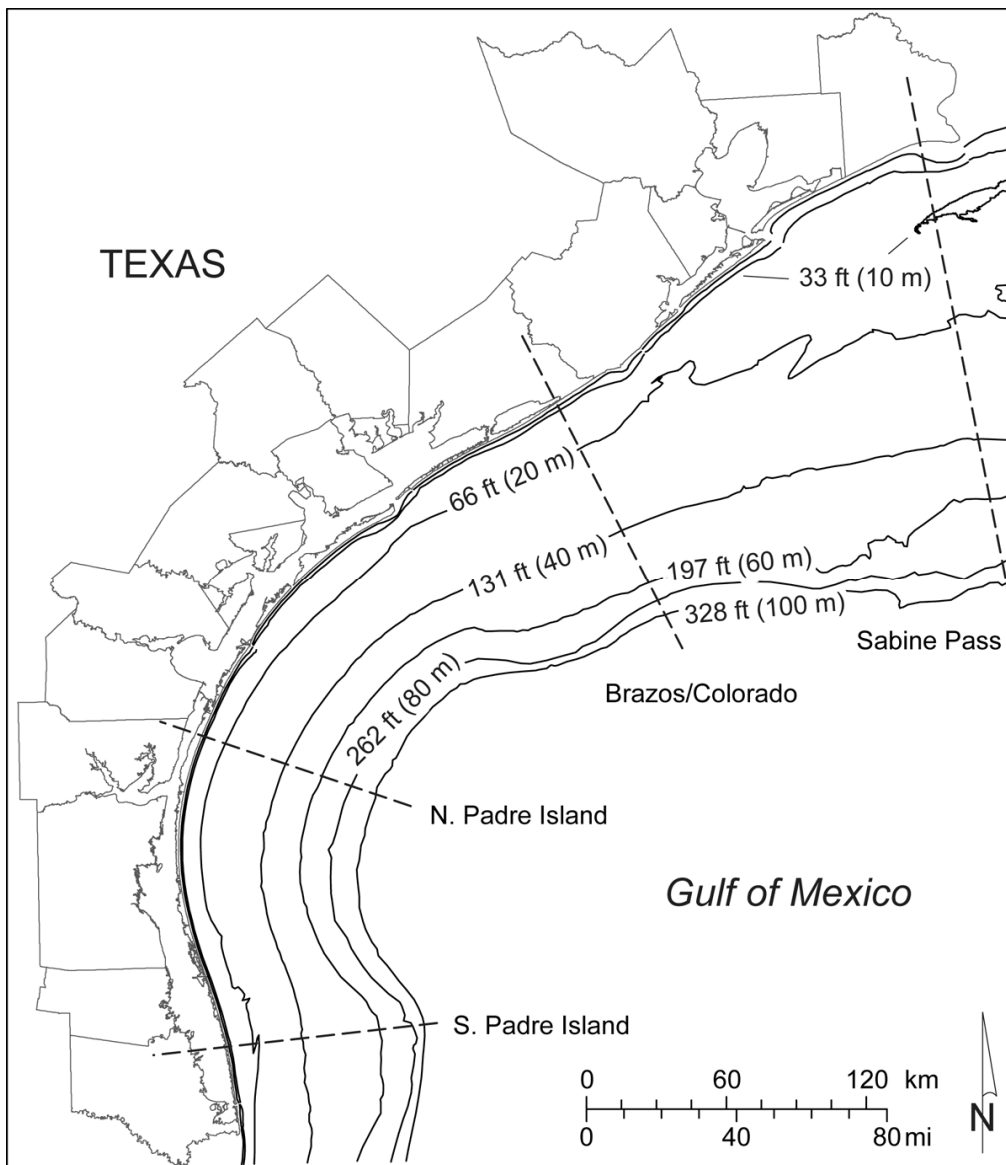


Figure 9. Major bathymetric contours on the Texas continental shelf and transect locations where postglacial net and interval shoreline migration rates are estimated using bathymetric contours as a shoreline proxy. Bathymetric data generalized from Holcombe and Arias (2009).

Table 4. Late Pleistocene and Holocene net shoreline retreat rates for the Texas coast estimated by assuming water depth (Fig. 9) approximates shoreline position at past sea-level positions. Effects of subsidence, sedimentation, and erosion are neglected and are significant sources of error. Sea-level ages and elevations are from northern Gulf of Mexico sea level curves published by Balsillie and Donoghue (2004, 2009) and Milliken et al. (2008).

Elev. (ft msl)	Age (ka)	Net rate to present (ft/yr)				Interval rate from previous position (ft/yr)			
		Sabine Pass	Brazos/Colorado	N. Padre Is.	S. Padre Is.	Sabine Pass	Brazos/Colorado	N. Padre Is.	S. Padre Is.
-20	7	-3.3	-0.7	-0.4	-0.4	-20.6	-6.4	-2.3	-2.7
-33	8	-5.4	-1.4	-0.6	-0.7	-108	-31.2	-14.3	-19.0
-66	10	-26.0	-7.4	-3.4	-4.3	-181	-132	-87.6	-60.0
-131	11	-40.1	-18.7	-11.0	-9.4	-44.6	-43.3	-26.7	-53.2
-197	13	-40.8	-22.5	-13.4	-16.2	-93.2	-28.2	-41.3	-45.6
-262	14	-44.6	-22.9	-15.4	-18.2	-15.9	-12.0	-18.4	-8.0
-328	16	-41.0	-21.6	-15.8	-17.0	-	-	-	-

- Coastal Research, v. 16, p. 111–124.
- Morton, R. A., 1974, Shoreline changes on Galveston Island (Bolivar Roads to San Luis Pass), an analysis of historical changes of the Texas Gulf Shoreline: Texas Bureau of Economic Geology Geological Circular 74–2, Austin, 34 p.
- Morton, R. A., 1975, Shoreline changes between Sabine Pass and Bolivar Roads: Texas Bureau of Economic Geology Geological Circular 75–6, Austin, 43 p.
- Morton, R. A., 1977, Historical shoreline changes and their causes, Texas Gulf Coast: Gulf Coast Association of Geological Societies Transactions, v. 27, p. 352–364. (Reprinted as Texas Bureau of Economic Geology Geological Circular 77–6, Austin, 13 p.)
- Morton, R. A., 1997, Gulf shoreline movement between Sabine Pass and the Brazos River, Texas: 1974 to 1996: Texas Bureau of Economic Geology Geological Circular 97–3, 46 p.
- Morton, R. A., M. P. Leach, and M. A. Cardoza, 1993, Monitoring beach changes using GPS surveying techniques: Journal of Coastal Research, v. 9, p. 702–720.
- Morton, R. A., T. L. Miller, and L. J. Moore, 2004, National assessment of shoreline change, part 1: Historical shoreline changes and associated coastal land loss along the U.S. Gulf of Mexico: U.S. Geological Survey Open-File Report 2004–1043, 42 p.
- Morton, R. A., and J. G. Paine, 1985, Beach and vegetation-line changes at Galveston Island, Texas: Erosion, deposition, and recovery from Hurricane Alicia: Texas Bureau of Economic Geology Geological Circular 85–5, Austin, 39 p.
- Morton, R. A., and J. G. Paine, 1990, Coastal land loss in Texas: An overview: Gulf Coast Association of Geological Societies Transactions, v. 40, p. 625–634.
- Morton, R. A., J. G. Paine, and J. C. Gibeaut, 1994, Stages and durations of post-storm beach recovery, southeastern Texas coast, U.S.A.: Journal of Coastal Research, v. 10, p. 884–908.
- Morton, R. A., and M. J. Pieper, 1975a, Shoreline changes on Brazos Island and South Padre Island (Mansfield Channel to mouth of the Rio Grande), an analysis of historical changes of the Texas Gulf shoreline: Texas Bureau of Economic Geology Geological Circular 75–2, Austin, 39 p.
- Morton, R. A., and M. J. Pieper, 1975b, Shoreline changes in the vicinity of the Brazos River delta (San Luis Pass to Brown Cedar Cut): Texas Bureau of Economic Geology Geological Circular 75–4, Austin, 47 p.
- Morton, R. A., and M. J. Pieper, 1976, Shoreline changes on Matagorda Island and San Jose Island (Pass Cavallo to Aransas Pass): Texas Bureau of Economic Geology Geological Circular 76–4, Austin, 42 p.
- Morton, R. A., and M. J. Pieper, 1977a, Shoreline changes on Mustang Island and North Padre Island (Aransas Pass to Yarborough Pass): Texas Bureau of Economic Geology Geological Circular 77–1, Austin, 45 p.
- Morton, R. A., and M. J. Pieper, 1977b, Shoreline changes on central Padre Island (Yarborough Pass to Mansfield Channel): Texas Bureau of Economic Geology Geological Circular 77–2, Austin, 35 p.
- Morton, R. A., M. J. Pieper, and J. H. McGowen, 1976, Shoreline changes on Matagorda Peninsula (Brown Cedar Cut to Pass Cavallo): Texas Bureau of Economic Geology Geological Circular 76–6, Austin, 37 p.
- Paine, J. G., 1991, Late Quaternary depositional units, sea level, and vertical movement along the central Texas coast: Ph. D. Dissertation, University of Texas at Austin, 256 p.
- Paine, J. G., 1993, Subsidence of the Texas coast: Inferences from historical and late Pleistocene sea levels: Tectonophysics, v. 222, p. 445–458.
- Paine, J. G., and R. A. Morton, 1989, Shoreline and vegetation-line movement, Texas Gulf Coast, 1974 to 1982: Texas Bureau of Economic Geology Geological Circular 89–1, Austin, 50 p.
- Paine, J. G., S. Mathew, and T. Caudle, 2011, Texas Gulf shoreline change rates through 2007: Final Report prepared by the Texas Bureau of Economic Geology for the General Land Office under Contract 10–041–000–3737, Austin, 38 p.
- Peltier, W. R., and A. M. Tushingham, 1989, Global sea level rise and the greenhouse effect: Might they be connected?: Science, v. 44, p. 806–810.
- Penland, S., and K. Ramsey, 1990, Sea-level rise in Louisiana and the Gulf of Mexico: 1908–1988: Journal of Coastal Research, v. 6, p. 323–342.
- Price, W. A., 1956, Hurricanes affecting the coast of Texas from Galveston to the Rio Grande: U.S. Army Corps of Engineers, Beach Erosion Board Technical Memorandum 78, Washington, DC, 35 p.
- Roth, D., 2010, Texas hurricane history: National Weather Service, Camp Springs, Maryland, 83 p., <<http://origin.hpc.ncep.noaa.gov/research/txhur.pdf>> Last Accessed September 10, 2012.
- Shalowitz, A. L., 1964, Shore and beach boundaries: U.S. Department of Commerce Publication 10–1, Washington, DC, 749 p.
- Simpson, R. H., and H. Riehl, 1981, The hurricane and its impact: Louisiana State University Press, Baton Rouge, 398 p.
- Swanson, R. L., and C. I. Thurlow, 1973, Recent subsidence rates along the Texas and Louisiana coast as determined from tide measurements: Journal of Geophysical Research, v. 78, p. 2665–2671.
- Thieler, E. R., E. A. Himmelstoss, J. L. Zichichi, and A. Ergul, 2009, Digital shoreline analysis system (DSAS) version 4.0—An ArcGIS extension for calculating shoreline change: U.S. Geological Survey Open-File Report 2008–1278, <<http://pubs.usgs.gov/of/2008/1278/>> Last Accessed August 22, 2012.